Int. J. Heat Mass Transfer. Vol. 32, No. 7, pp. 1299–1308, 1989
Printed in Great Britain

0017–9310/89 $3.00 + 0.00

Unsteady vaporization of stationary dodecane and alcohol droplets suspended in a hot non-reactive environment

M. M. MEGAHED,† M. N. SAEED,† M. M. SOROUR‡ and M. B. MADI†

†Department of Mechanical Engineering, Alexandria University, Alexandria, Egypt
‡Department of Mechanical Engineering, Sultan Qaboos University, Oman

(*Received* 18 *May* 1988 *and in final form* 22 *November* 1988)

Abstract—A computer model is developed to calculate the transport properties of a single droplet during vaporization in heterogeneous combustion systems. A fourth-order Runge–Kutta technique determines the liquid phase properties and the film properties in terms of time. The model computes the history of droplet size, temperature, vapour pressure, rate of mass vaporization, rates of heat transfer and heat flux, and cumulative values of both evaporated mass and heat transfer. A new approach is presented in this investigation for calculating the evaporation constant of single droplets. The results presented show that the use of alcohols as alternate fuels in heterogeneous combustion systems requires higher chamber temperatures and smaller droplets in order to keep the vaporization time within the acceptable range.

INTRODUCTION

SPRAY VAPORIZATION is of primary importance in predicting and improving the performance of systems utilizing spray injection such as gas turbines, rocket motors and compression-ignited engines. Vaporization of fuel droplets takes place during the physical ignition delay period, which is defined by El-Wakil *et al.* [1] as the time required to form a stoichiometric mixture in the vapour film surrounding the liquid droplet. Henein [2] modified this definition by specifying the location of the stoichiometric mixture to be on the droplet surface rather than within the film. Since droplet vaporization affects the concentration of the combustible mixture, the temperature of the combustion chamber, and the reaction kinetics responsible for exothermic reactions, the study of heat and mass transfer of vaporizing liquid droplets is essential.

Droplet vaporization models have been classified into two major categories: spherical-symmetry models and axisymmetric models [3]. The first of the spherical-symmetry models is the famous d^2-law model, which assumes a linear relationship between the droplet surface area and time [3–7]. Aggarwal *et al.* [3] used the d^2-law for studying hexadecane, decane and hexane. Hiroyasu *et al.* [6] and later Kadota and Hiroyasu [7] followed the same model for investigating a number of hydrocarbons as well as ethanol and water. Nishiwaki [4] noticed that the relationship between the droplet surface area and time is not linear. He therefore divided the relationship into segments of straight lines. A modification to the d^2-law model is the infinite-conductivity model [3], in which the assumption of the constant liquid-phase temperature is replaced by a uniform time-dependent droplet temperature. Sirignano [8] showed that the uniform temperature is a result of the infinite conductivity. Henein [2] applied the same model to iso-octane, and found the results to be in good agreement with Faeth's experiments [9]. The third of the spherical-symmetry models is the conduction-limit model [3, 10]. This model neglects the internal circulation within the droplet, and results in a non-uniform temperature distribution. Because of the complexities of that model, simplified assumptions such as average liquid-phase and vapour-phase properties are usually made [10]. The soundness of such an assumption is questionable when the droplet temperature undergoes fast variations. Aggarwal *et al.* [3] compared the results of both the infinite-conductivity model and the conduction-limit model, and found that both models predict about the same droplet lifetime. On the other hand, Prakash and Sirignano [11, 12] developed a two-dimensional axisymmetric model in order to study the cases in which the Reynolds number is very large compared to unity. Although the axisymmetric model is one of the most detailed as well as accurate models in the case of inviscid fluids, it is not yet tested in the case of real fluids [3]. Tong and Sirignano [14, 15] simplified the axisymmetric model, and found the accuracy of the results still acceptable.

The aforementioned review reveals that although many investigations have been conducted on single-component vaporization of conventional fuels, little has been done in the vaporization process of alcohols in heterogeneous combustion systems. As a result of the energy crises of 1973 and 1979, alcohols were looked upon as promising alternative fuels [16]. Alcohols can be distilled from abundant renewable resources such as woods, sugar cane, barley and corn. They can be synthesized from gases like carbon di-

NOMENCLATURE

a	constant used in equation (16)
b	constant used in equation (16)
C_L	liquid phase specific heat
$\bar{h}$	average heat transfer coefficient
h_{fg}	latent heat of vaporization
K	evaporation constant
K_{600}	evaporation constant at $T_\infty = 600$ K
$\bar{k}$	vapour film thermal conductivity
M	mass
M_{ev}	evaporated mass
M_0	initial mass at $t = 0$
m_{cv}	mass of control volume
m_L	mass of liquid phase
m_v	mass of vapour phase
n	exponent used in equation (12)
$\overline{Nu}$	average Nusselt number
Pr	Prandtl number
Q	heat energy
Q_L	latent heat transfer
Q_s	sensible heat transfer
Q_t	total heat transfer
R	droplet radius at time t
R_0	droplet radius at $t = 0$
Re	Reynolds number
T_{eq}	equilibrium temperature
T_∞	surrounding temperature
T_L	temperature of liquid droplet
T_{L0}	temperature of liquid droplet at $t = 0$
t	time
t^*	time of complete vaporization
X	any property.

Greek symbols

β	exponent used in equation (9)
ρ_L	density of liquid droplet.

oxide and hydrogen. Because alcohols have octane numbers higher than 90, they have been proven superior for powering spark-ignited engines. However, alcohols still constitute a considerable challenge for use in heterogeneous combustion systems, owing to their low cetane numbers, large latent heat of vaporization, and long ignition delays [16].

The few studies conducted on vaporization of alcohol droplets were concerned with either the history of the droplet surface area or the physical ignition delay of the droplet. Nishiwaki [4] investigated the vaporization of both methanol and ethanol experimentally and theoretically. He assumed that the relation between the surface area and time could be divided into segments of straight lines the slopes of which were the evaporation constants. Hiroyasu and Kadota [6, 7] determined, both experimentally and theoretically, an overall evaporation constant for ethanol that was based on the d^2-law. Reference [17] dedicated its theoretical investigation to the physical ignition delay of ethanol droplets. Details of heat and mass transfer were not the focus of ref. [17].

A computer model based on the infinite-conductivity hypothesis has been developed. The model is valid for a wide range of fuels since it uses temperature-dependent property equations written in terms of molecular mass, molecular structure, critical constants and temperature. Histories of droplet size, droplet temperature, heat transfer, heat flux and rate of mass evaporation are predicted. The alcohols under investigation are methanol, ethanol and isopropanol. The temperature range is 600–1000 K. The results are presented and compared with vaporization characteristics of dodecane (a pure hydrocarbon the auto-ignition characteristics of which resemble those of diesel fuel). A new approach is developed for the determination of an overall evaporation constant that takes into account the deviation from the d^2-law.

ANALYSIS

Formulation of the problem

The fuel droplet is assumed spherical throughout its lifetime. In order to isolate the effect of flames on vaporization, the droplet is treated as if it were suspended in stagnant nitrogen. The interaction between neighbouring droplets is neglected. No concentration or temperature gradients exist within the droplet. The thickness of the vapour film surrounding the droplet is assumed to be of the order of magnitude of the droplet radius. Based on the investigations reported in the literature [2, 9, 22, 23], the average properties of the fuel–vapour film do not exist in the middle of the film, but rather are close to the droplet surface (30–40% of film thickness). The logarithmic mean may therefore be more realistic for defining the average temperature of the film than the arithmetic mean. The total heat Q_t transferred from the hot gas to the droplet can be divided, in the absence of radiative terms, into sensible heat Q_s and latent heat Q_L. The conservation of mass yields

$$dm_{cv}/dt + dm_v/dt = 0. \quad (1)$$

Since the control volume contains only the liquid phase, $m_{cv} = m_L$ and

$$dm_{cv}/dt = dm_L/dt = -dm_v/dt. \quad (2)$$

The rate of change dm_L/dt is determined by

$$dm_L/dt = \frac{d}{dt}\left(\frac{4}{3}\pi R^3 \rho_L\right). \quad (3)$$

For $R^3(\mathrm{d}\rho_L/\mathrm{d}t) \ll 3\rho_L R^2(\mathrm{d}R/\mathrm{d}t)$, equation (3) may be rewritten as

$$\mathrm{d}m_L/\mathrm{d}t = 4\pi\rho_L R^2(\mathrm{d}R/\mathrm{d}t). \quad (4)$$

The heat flow rate absorbed through the droplet surface is equal to the rate of change of droplet internal energy plus the rate of energy used for evaporating an incremental volume of the liquid phase, i.e.

$$4\pi R^2\bar{h}(T_\infty - T_L) = \tfrac{4}{3}\pi R^3\rho_L C_L(\mathrm{d}T_L/\mathrm{d}t) - 4\pi R^2\rho_L h_{fg}(\mathrm{d}R/\mathrm{d}t). \quad (5)$$

Equation (5) holds as long as

$$R(\mathrm{d}X/\mathrm{d}t) \ll X(\mathrm{d}R/\mathrm{d}t)$$

where X is any liquid property ρ_L, C_L, T_L or h_{fg}. The mean heat transfer coefficient $\bar{h}$ is given by Ranz and Marshall [18] as

$$\overline{Nu} = \bar{h}(2R)/\bar{k} = 2 + 0.6Re^{1/2}Pr^{1/3}. \quad (6)$$

From the assumption that the relative velocity of the droplet with respect to the surrounding gas is negligible, $Re \to 0$ and equation (6) becomes

$$\bar{h} = \bar{k}/R. \quad (7)$$

Moreover, energy equation (5) can be rewritten in terms of $\bar{k}$ as

$$\mathrm{d}R/\mathrm{d}t = \tfrac{1}{3}R(C_L/h_{fg})(\mathrm{d}T_L/\mathrm{d}t) - (\bar{k}/(R\rho_L h_{fg}))(T_\infty - T_L). \quad (8)$$

Solution methodology

Assuming constant-pressure surroundings, the physical properties of both the droplet and the surrounding film depend mainly on temperature. The history of droplet temperature may be described by the following equation, the form of which was introduced by Henein [2] in 1971:

$$T_L = T_{eq} - (T_{eq} - T_{L0})\exp(-\beta t). \quad (9)$$

The equilibrium temperature T_{eq} is defined as the temperature of the liquid droplet at which all the energy reaching the droplet surface is used for evaporating the liquid phase; in other words, it is the temperature at which $\mathrm{d}T_L/\mathrm{d}t = 0$ (in case of atmospheric pressure, T_{eq} corresponds to the liquid boiling temperature). Since the properties $\bar{k}$, ρ_L, h_{fg} and C_L of equation (8) are temperature dependent, and since the temperature T_L is time dependent (according to equation (9)), the rate of change of droplet radius $\mathrm{d}R/\mathrm{d}t$ of equation (8) can be expressed in the following general form:

$$\mathrm{d}R/\mathrm{d}t = F(R, t) \quad (10)$$

which is a first-order ordinary differential equation that can be solved numerically by using a fourth-order Runge–Kutta technique.

The constant β in equation (9) is determined according to ref. [16] by

$$\beta = ((3\bar{k}/(R^2\rho_L C_L))(T_\infty - T_L)/(T_{eq} - T_L) + (3h_{fg}/(RC_L(T_{eq} - T_L)))(\mathrm{d}R/\mathrm{d}t))_{t=0}. \quad (11)$$

The derivation of equation (11) is presented in the Appendix. Knowing the values of T_{eq} and β, the history of liquid droplet temperature T_L can be determined from equation (9). The Runge–Kutta technique determines the liquid phase properties and the film properties in terms of time. The instantaneous rate of change of droplet radius $\mathrm{d}R/\mathrm{d}t$ is calculated from equation (8). This rate is used for determining the radius after an incremental time $\mathrm{d}t$, and so forth. The equations used for calculating properties are presented in refs. [19, 20].

Validation of the model

A computer program was developed and run using a suitable time increment for computations. The program was then re-run using a smaller time increment (usually 50% of the first increment). The values of $\mathrm{d}M/\mathrm{d}t$ and $\delta Q/\delta t$ for both runs were compared. If the error was not more than 3%, computations were terminated. Otherwise, a smaller time increment was used, and a new history of vaporization was calculated. The reason for selecting $\mathrm{d}M/\mathrm{d}t$ and $\delta Q/\delta t$ to verify the accuracy of computations is simple: since the mass rate of vaporization and the rate of heat transfer depend on the droplet size and the properties of both liquid and gas phases, by setting the error in computing $\mathrm{d}M/\mathrm{d}t$ and $\delta Q/\delta t$ at 3%, the computational error for properties must be less than 3%. The end of vaporization was defined by the time when the droplet mass was less than or equal to 2% of the initial droplet mass.

The range of validity of the present model was determined by comparing the present results with the previous experimental results of other investigators [2, 9, 21]. Figure 1(a) compares the histories of droplet temperature as determined by the present model, the experimental results of Faeth [9] and the theoretical results of Henein [2]. (The initial radius of the octane droplet is 570 μm. The initial droplet temperature is 287 K, and the temperature of the hot gas is 863 K.) It is obvious from Fig. 1(a) that the present model agrees with Faeth's experimental results [9]. On the other hand, the comparison with Henein's work [2] shows a growing deviation that may be caused by the constant-property, constant-diameter assumption that Henein used (the assumption is similar to the porous-sphere case in which the rate of fuel supplied to the sphere is equal to the rate of vaporization). Although this assumption is acceptable at the beginning of vaporization, the error will accumulate as time elapses. According to equation (7), the heat transfer coefficient is inversely proportional to the droplet radius. Henein's assumption will therefore result in a lower-than-actual heat transfer coefficient and, consequently, Henein's solution [2] predicts temperatures that are 10 K lower than those measured by Faeth [9].

Another way of validating the model is by comparing the history of droplet surface area with experimental data. Figure 1(b) shows the present results

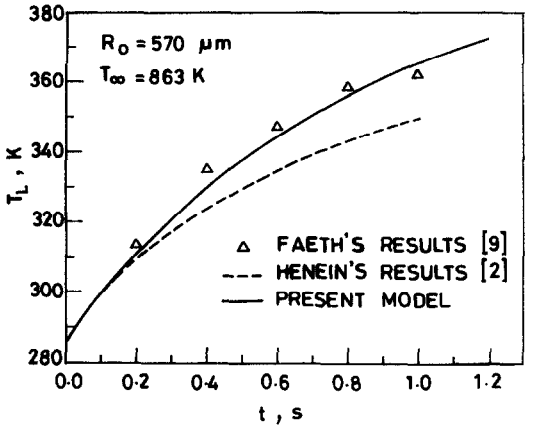

(a)

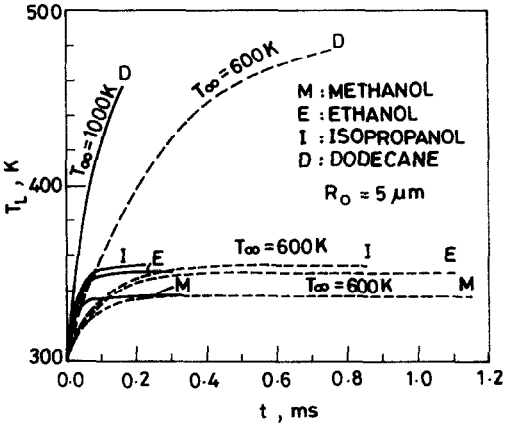

FIG. 2. History of droplet temperature.

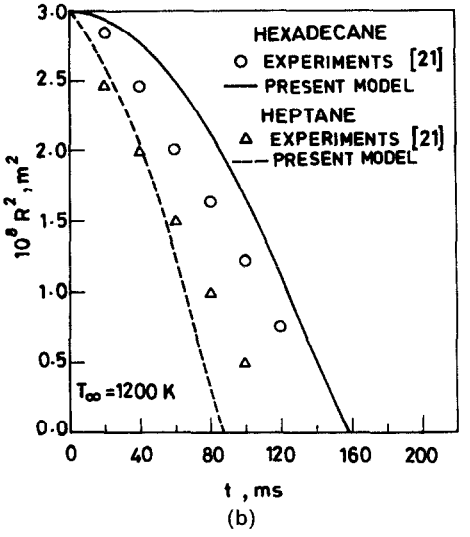

(b)

FIG. 1. (a) Present model vs results by Henein [2] and Faeth [9]. (b) Present model vs results by Wang *et al.* [21].

against the experimental results by Wang *et al.* [21] at 0.1 MPa and 1200 K. It appears from the figure that the present model predicts a longer time for hexadecane droplets to shrink to a certain surface area. The difference is explained by the fact that the present model is based on fuel droplets suspended in nitrogen, while the experiments reported by Wang *et al.* [21] were conducted on fuel droplets suspended in air. The vaporization rate in the case of a burning droplet must therefore be higher than that for a droplet vaporizing in the absence of flames. The heptane droplets, on the other hand, show a longer time at the beginning of vaporization and a shorter time near the end of vaporization. This shorter time may have been caused by a slight overestimation of the film thermal conductivity, and thus increasing the predicted values of the heat transfer coefficient and the rate of heat transferred to the heptane droplet. The maximum and average errors in predicting the history t for a certain R^2 are, respectively, 55 and 35% for hexadecane, and 24 and 16% for heptane.

Based on the above comparisons and the range of validity of the equations used for calculating thermophysical properties, the present model may be suitable for predicting the history of droplet vaporization under the following conditions: the droplet diameter being under 1 mm, the surrounding temperature being between 700 and 1200 K, and the vaporization process taking place in the absence of flames.

DISCUSSION OF RESULTS

Figure 2 shows the history of droplet temperature starting from the time at which the droplet is placed into an environment of hot nitrogen. The figure compares dodecane with three alcohols: isopropanol, ethanol and methanol. At $T_\infty = 1000$ K, the time needed for complete vaporization ranges from 130 μs for dodecane to 325 μs for methanol. This may be explained by the latent heat of vaporization, which is the smallest for dodecane and the greatest for methanol. The figure shows the alcohols acquire sensible heating during the first stage of vaporization, which ends as the droplet reaches its equilibrium temperature. The second stage is a constant-temperature vaporization, which ends as the droplet is completely vaporized. Dodecane, on the other hand, does not show this two-stage behaviour because of its relatively small latent heat. As for the effect of chamber temperature T_∞, Fig. 2 shows that increasing the temperature from 600 to 1000 K would shorten the vaporization time tremendously. This is due to the resulting increase in the rate of heat transfer.

The variation of heat flux for various system parameters is presented in Fig. 3. It appears from Fig. 3(a) that the heat flux develops a local maximum followed by a local minimum, then explodes as the droplet radius diminishes. Initially, the film thermal conductivity increases as the droplet temperature rises with time. During this initial stage of sensible heating, there is no significant change in the droplet radius. Therefore, the heat transfer coefficient $\bar{h}$ increases (according to equation (7)), and so does the heat flux. However, at a further stage, the drop in the heat

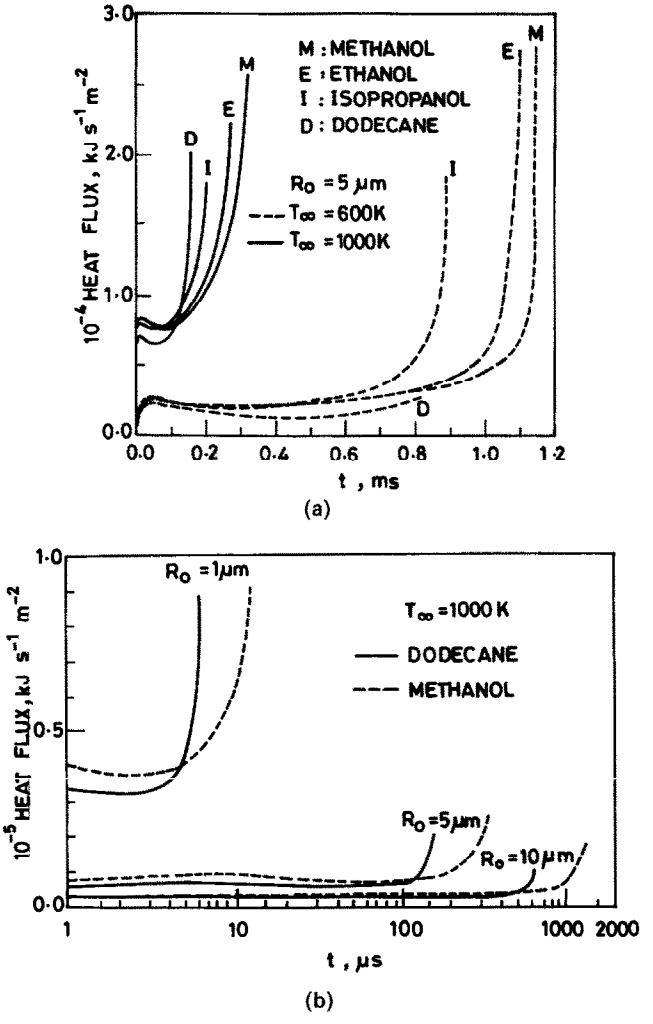

FIG. 3. (a) Effect of surrounding temperature on heat flux history. (b) Effect of droplet size on the history of heat flux.

transfer rate associated with the shrinking droplet causes the heat flux to fall off its local maximum, but at a slow rate. This fall continues until the effect of droplet shrinkage becomes predominant, and the heat flux reaches a local minimum. With further vaporization, the droplet radius diminishes rapidly, resulting in sharp increases in both the heat transfer coefficient $\bar{h}$ and the heat flux. For the same conditions, the dodecane droplet shows the earliest shootup in heat flux since it is the fastest to vaporize. In addition, increasing the chamber temperature T_∞ increases both the rate of heat transfer and the heat flux. Lastly, the heat flux becomes very low with larger fuel droplets, resulting in longer vaporization time, as shown in Fig. 3(b).

The latent heat effect is pronounced in Fig. 4(a) which shows both sensible and total heat transfer. The difference in ordinates between Q_t and Q_s is the latent heat transfer Q_L. The figure shows clearly that the latent heat transfer constitutes over 80% of the total heat transfer in the case of methanol vaporization. On the other hand, the fraction is only about 30% in the case of dodecane. The peak rate of heat transfer which is observed in the figure can be explained as follows. During the early stage of vaporization, the droplet temperature increases, and so does the film temperature. Because the film thermal conductivity $\bar{k}$ increases with temperature, and the heat transfer coefficient $\bar{h}$ increases with $\bar{k}$ (according to equation (7)), the heat transfer increases. Later on, further increase in droplet temperature causes the thermal gradient to taper off, and the heat transfer rate to decrease.

The rate of vapour formation dM/dt is presented in Fig. 4(b). The figure shows that all fuels yield an increasing rate up to a maximum, then the rate slows down till the end of vaporization. The greatest rate of vapour formation is for dodecane droplets, followed by isopropanol, ethanol and methanol. This behaviour is closely related to the rate of heat transfer shown in Fig. 4(a) and its similar behaviour. In the beginning, the rate of heat transfer increases, and so does the rate of vapour formation. Later on, the rate of heat transfer decreases, leading to a decreasing rate of

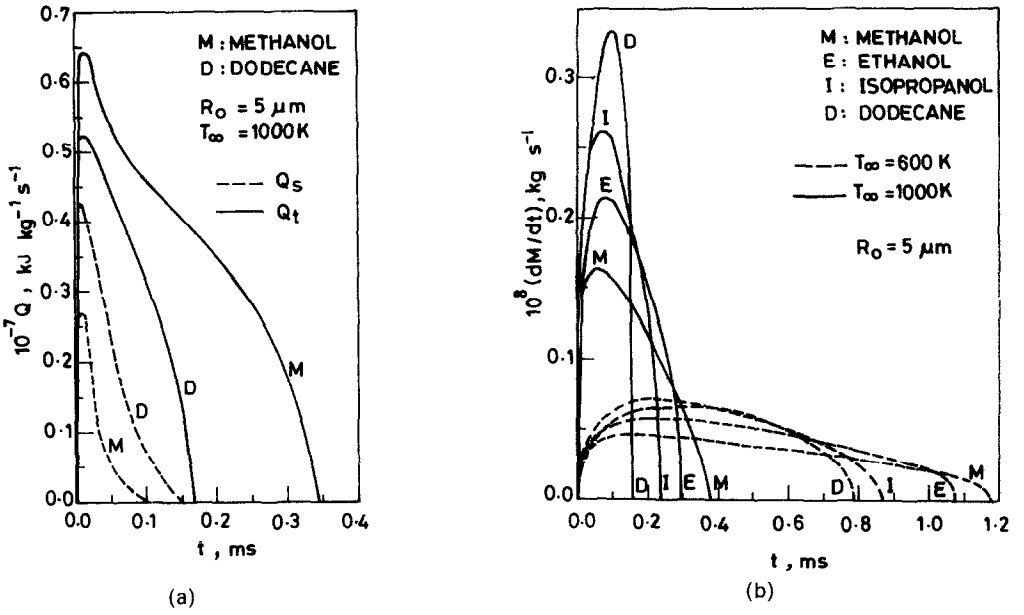

FIG. 4. (a) Effect of fuel type on history of heat transfer. (b) Effect of fuel type on history of mass vaporization rate.

vapour formation. The maximum rates of vapour formation depend mainly on the latent heat of vaporization; the smaller the latent heat, the higher the maximum rate $(dM/dt)_{max}$. The effect of chamber temperature T_∞ on the rate of vapour formation is also presented in Fig. 4(b). It is clear that increasing the temperature T_∞ from 600 to 1000 K raises the rate of heat transfer, and the vaporization rate consequently increases.

Figure 5 shows the effects of fuel type, droplet size and chamber temperature on the ratio of the evaporated mass M_{ev} to the initial mass M_0. It is obvious that M_{ev}/M_0 increases sharply with time in the case of dodecane. The rate of increase is slower for isopropanol, followed by ethanol and methanol. Since the heat energy consumed by unit mass of the droplet is inversely proportional to the droplet surface area, the ratio M_{ev}/M_0 is the steepest for small droplets ($R_0 = 1$ μm). In addition, the temperature T_∞ influences the ratio M_{ev}/M_0 in the same way it influences the rate dM/dt—i.e. the higher the temperature, the greater the ratio M_{ev}/M_0. Lowering the chamber temperature T_∞ from 1000 to 600 K would have the same effect on M_{ev}/M_0 as increasing the droplet radius from 5 to 10 μm.

An interesting relationship between the dimensionless evaporated mass and dimensionless time is shown in Fig. 6. The hypothetical line with unit slope represents linear vaporization, i.e. the fraction evaporated is exactly equal to the time fraction t/t^*.

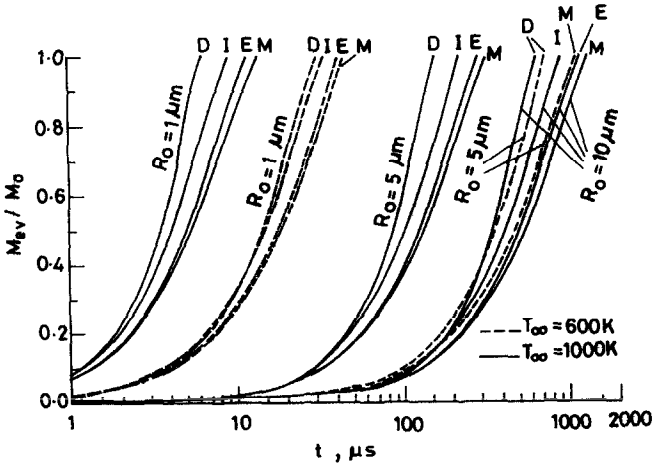

FIG. 5. History of fraction of mass evaporated.

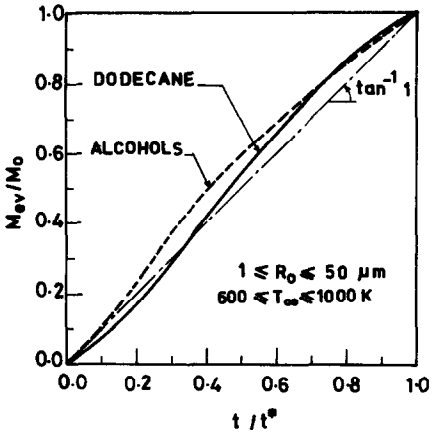

FIG. 6. Non-dimensional history of fraction of mass evaporated.

However, the curves representing dodecane and alcohols show deviations from the unit-slope line. The line for alcohols always satisfies the condition $(M_{ev}/M_0) > (t/t^*)$ except at $t/t^* = 0$ and 1. This may be explained by the high volatility of alcohols, which is a driving force for evaporation. On the other hand, the dodecane line satisfies the condition $(M_{ev}/M_0) < (t/t^*)$ up to $t/t^* = 0.34$. The trend then changes such that $(M_{ev}/M_0) > (t/t^*)$ till the end of vaporization. Sensible heating is what dodecane acquires during the first stage of vaporization. The role of latent heating becomes predominant in the second stage, and the dodecane line is, therefore, lower than the unit-slope line for $(t/t^*) < 0.34$ and higher than it for $(t/t^*) > 0.34$.

The logarithmic relation between the vaporization time t^* and the droplet initial radius R_0 is shown in Fig. 7 for the fuels investigated at $T_\infty = 600$ and 1000 K. It is interesting to note that all cases show a straight-line relationship of the same slope—2. This means that the vaporization time is directly proportional to the droplet surface area. Because the heat

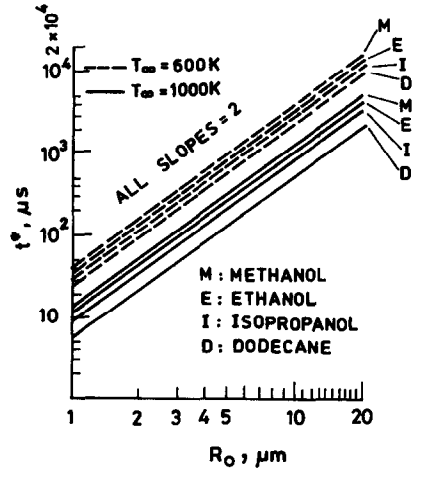

FIG. 7. Total lifetime of droplets of various sizes and fuels.

transfer coefficient $\bar{h}$ is proportional to R_0^{-1} in the case of a droplet suspended in stagnant gas, the rate of heat transfer to the droplet will be proportional to R_0^2 times R_0^{-1}, and the rate of heat transfer per unit mass of the liquid droplet will be proportional to R_0^2 times R_0^{-1} times R_0^{-3}. The rate of temperature rise for the liquid droplet will therefore be proportional to R_0^{-2}, and the time required for vaporizing the droplet will be proportional to R_0^2. On the other hand, in the case of a moving droplet, the heat transfer coefficient is proportional to $R_0^{-0.5}$ because the Nusselt number is approximately proportional to the square root of the Reynolds number, which is proportional to R_0. The resulting rate of temperature rise for the droplet will be proportional to $R_0^{-1.5}$, and the vaporization time will be proportional to $R_0^{1.5}$. The results found by El-Wakil *et al.* [1] were $t^* \propto R_0^{1.75}$.

Evaporation constant K

The evaporation constant K is evaluated in the present work by using a modified form of the d^2-law [3–7]. This approach takes into account the nonlinearity encountered in the relation between time and the droplet surface area. The proposed equation is

$$R^2 = R_0^2 - Kt^{*1-n}t^n. \tag{12}$$

The normalized form of equation (12) may be written as

$$1-(R/R_0)^2 - (Kt^*/R_0^2)(t/t^*)^n. \tag{13}$$

Keeping in mind that R_0^2/Kt^* is equal to unity, according to equation (12), the logarithmic form of equation (13) is

$$\ln(1/(1-(R/R_0)^2)) = n \ln(t^*/t). \tag{14}$$

The non-dimensional constant n can be determined from the linear relationship between $\ln(t^*/t)$ and $\ln(1/(1-(R/R_0)^2))$. From equation (12), the evaporation constant K is determined by

$$K = R_0^2/t^*. \tag{15}$$

On the other hand, the exponent n represents the slope of equation (14). It was found that the value of n is independent of the temperature T_∞ and the droplet radius R_0, but it depends mainly on the fuel type. The highest value of n is 1.79 in the case of dodecane. Isopropanol, ethanol and methanol have the values 1.41, 1.33 and 1.27, respectively. Figure 8 shows logarithmic plots of equation (12) for the four fuels.

According to equation (15), the evaporation constant K depends on both the initial radius R_0 and the time of complete vaporization t^*. Since t^* depends on the fuel type, surrounding temperature T_∞ and R_0, the value of K must depend on R_0, T_∞ and the fuel type. However, the ratio R_0^2/t^* cancels out the dependency of K on R_0. Figure 9 shows that for $1 < R_0 < 20$ μm, each fuel has its own K–T_∞ relationship. It appears that the evaporation constant is the greatest for dodecane and the smallest for methanol, and that the surrounding temperature T_∞ enhances its value

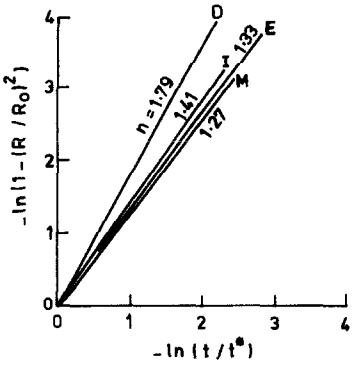

FIG. 8. Logarithmic plots of equation (12).

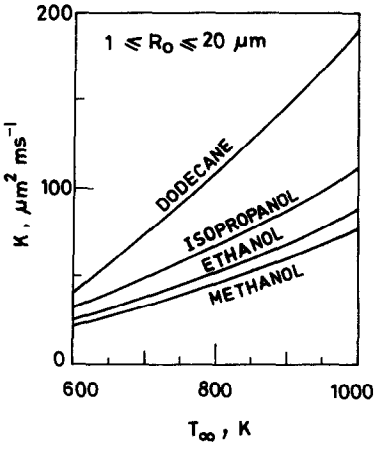

FIG. 9. Evaporation constant for dodecane and alochol fuels.

for all fuels investigated. The K–T_∞ relationship may be written as

$$K - K_{600} = a((T_\infty - 600)/400)^b \qquad (16)$$

provided that $600 \leqslant T_\infty \leqslant 1000$ K. The values of a, b and K_{600} are given in Table 1.

The present values of the evaporation constant for ethanol appear to be smaller than those values reported in the literature. Nishiwaki [4] reported experimental values of $K = 130$ and 220 μm^2 ms^{-1} for droplet diameters of 0.55 and 1 mm, respectively. Kobayasi [25] reported experimental values of $K = 900$ μm^2 ms^{-1} for droplets having diameters between 0.7 and 1.7 mm. Godsave [5] determined experimentally the evaporation constant as 800 μm^2 ms^{-1} for droplets of 1.5 mm diameter. The difference between the present work and the above studies may be attributed to the fact that all of the above experiments were conducted in the presence of flames, while the present study is concerned with droplets suspended in non-reactive environments. On the other hand, the values of the evaporation constant as experimentally determined by Hiroyasu *et al.* [6] in an environment of nitrogen are approximately eight times greater than the values found by the present investigation. This latter finding is not a surprise, since the heat transfer to Hiroyasu's droplets was, to a great extent, by conduction. The droplets were attached to their solid droplet maker and the whole apparatus was immersed in a high temperature environment at 500°C (773 K).

Table 1. Constants of equation (16)

	a (μm^2 ms^{-1})	b	K_{600} (μm^2 ms^{-1})
Dodecane	150	1.070	40
Isopropanol	80	1.085	31
Ethanol	64	1.115	24
Methanol	54	1.134	22

CONCLUSIONS

A new approach is presented for calculating the evaporation constant of single droplets. Numerical values of the evaporation constant for various fuels can be determined, in terms of the combustion-chamber temperature, by equation (16).

The present study indicates the scope with which alcohols can be used as alternate fuels in heterogeneous combustion systems. Higher chamber temperatures and smaller droplets must be attained in order to keep the vaporization time within the acceptable range.

Further investigations are recommended through both analytical and experimental avenues in order to develop more accurate models.

REFERENCES

1. M. M. El-Wakil, P. S. Myers and O. A. Uyehara, Fuel vaporization and ignition lag in diesel combustion, *SAE Trans.* **64,** 712–729 (1956).
2. N. A. Henein, A mathematical model for the mass transfer and combustible mixture formation around fuel droplets, SAE Paper 710221 (1971).
3. S. K. Aggarwal, A. Y. Tong and W. A. Sirignano, A comparison of vaporization model in spray calculations, *AIAA J.* **22**(10), 1448–1457 (1984).
4. N. Nishiwaki, Kinetics of liquid combustion processes: evaporation and ignition lag of fuel droplets, Fifth Symp. (Int.) on Combustion, pp. 148–158 (1954).
5. G. A. E. Godsave, Studies of the combustion of drops in a fuel spray—the burning of single drops of fuel, Fourth Symp. (Int.) on Combustion, pp. 818–830 (1952).
6. H. Hiroyasu, T. Kadota, T. Senda and T. Imamoto, Evaporation of a single droplet at elevated pressures and temperatures (experimental study), translated from *JSME Trans.* **40,** 3147 (1974).
7. T. Kadota and H. Hiroyasu, Evaporation of a single droplet at elevated pressures and temperatures (2nd report, theoretical study), *JSME* **19,** 138 (1976).
8. W. A. Sirignano, Theory of multi-component fuel droplet vaporization, *Arch. Thermodynam. Combust.* **9**(2), 231–247 (1978).
9. G. M. Faeth, The kinetics of droplet ignition in a quiescent air environment, Ph.D. Dissertation, The Pennsylvania State University (1964).
10. C. K. Law and W. A. Sirignano, Unsteady droplet com-

bustion with droplet heating—II. Conduction limit, *Combust. Flame* **28**, 175–186 (1977).
11. S. Prakash and W. A. Sirignano, Theory of convective droplet vaporization with unsteady heat transfer in the circulating liquid phase, *Int. J. Heat Mass Transfer* **23**(3), 253–268 (1980).
12. S. Prakash and W. A. Sirignano, Liquid fuel droplet heating with internal circulation, *Int. J. Heat Mass Transfer* **21**, 885–895 (1978).
13. J. D. Jin and G. L. Borman, A model for multicomponent droplet vaporization at high ambient pressures, SAE Paper 850264 (1985).
14. A. Y. Tong and W. A. Sirignano, Analytical solution for diffusion in the core of a droplet with internal circulation, AIChE Symp. Series, Heat Transfer, Milwaukee, pp. 400–407 (1981).
15. A. Y. Tong and W. A. Sirignano, Analysis of vaporizing droplet with slip, internal circulation and unsteady liquid phase heat transfer, JSME–ASME Thermal Engng Joint Conf., Honolulu, Hawaii (1983).
16. M. N. Saeed, Combustion characteristics of neat ethanol and blends of ethanol and diesel fuel number two in a direct-injection diesel engine, Ph.D. Dissertation, Wayne State University (1984).
17. M. N. Saeed and N. A. Henein, Physical ignition delay for ethanol droplets in diesel engines, ASME Paper 87-Pet-4 (1987).
18. W. E. Ranz and W. R. Marshall, Evaporation from drops, *Chem. Engng Prog.* **48**(3), 141–148 (1952).
19. R. C. Reid, J. M. Prausnitz and T. K. Sherwood, *The Properties of Gases and Liquids* (3rd Edn). McGraw-Hill, New York (1977).
20. M. M. Megahed, Multicomponent droplet vaporization and its application to alcohol–dodecane mixtures, M.Sc. Thesis, Alexandria University (1988).
21. C. H. Wang, X. Q. Liu and C. K. Law, Combustion and microexplosion of freely falling multicomponent droplets, *Combust. Flame* **56**, 175–197 (1984).
22. M. M. El-Wakil, O. A. Uyehara and P. S. Myers, A theoretical investigation of the heating-up period of injected fuel droplets vaporizing in air, NACA Tech. Note 3179 (1954).
23. M. N. Saeed, An exact solution to the unsteady mass diffusion of vaporizing liquid fuel drops, ASME Paper 86-WA/FACT-7, Winter Annual Meeting, Anaheim, California, 7–12 December (1986).
24. D. B. Spalding, The combustion of liquid fuels, Fourth Symp. (Int). on Combustion, pp. 847–864 (1952).
25. K. Kobayasi, An experimental study on the combustion of a fuel droplet, Fifth Symp. (Int.) on Combustion, pp. 141–148 (1954).

APPENDIX. DERIVATION OF EQUATION (11)

(1) By differentiating equation (9), one obtains

$$dT_L/dt = \beta(T_{eq} - T_{L0}) \exp(-\beta t)$$
$$= \beta(T_{eq} - T_L).$$

(2) Substituting the result of step 1 into equation (8) for $(dR/dt)_{t=0} = 0$, the first approximation of β is given by

$$\beta = ((3\bar{k}(R^2\rho_L C_L))(T_\infty - T_L)/(T_{eq} - T_L))_{t=0}.$$

(3) The first approximation of β is used for calculating the size of the droplet after an incremental time Δt. The value of $(\Delta R/\Delta t)$ can now be estimated near $t = 0$.

(4) Using this latter value of $(\Delta R/\Delta t)$ as a new value of $(dR/dt)_{t=0}$, a better approximation of β is calculated from equation (8) as

$$\beta = ((3\bar{k}/(R^2\rho_L C_L))(T_\infty - T_L)/(T_{eq} - T_L) + (3h_{fg}/(RC_L(T_{eq} - T_L)))(dR/dt))_{t=0}.$$

(5) Steps 3 and 4 are repeated until a sufficiently stable value of β is obtained.

VAPORISATION VARIABLE DE GOUTTELETTES DE DODECANE ET D'ALCOOL DANS UN ENVIRONNEMENT CHAUD ET NON REACTIF

Résumé—Un modèle permet le calcul des propriétés de transport d'une gouttelette unique pendant la vaporisation dans des systèmes de combustion hétérogène. Une technique de Runge–Kutta du quatrième ordre détermine les propriétés de la phase liquide et celles du film en fonction du temps. Le modèle calcule l'histoire de la taille de la goutte, de la température, de la pression de vapeur, du flux de masse vaporisée, du flux de chaleur transférée et des valeurs cumulées de la masse et de la chaleur transférées. On présente une nouvelle approche dans cette étude pour calculer la constante d'évaporation des gouttelettes. Les résultats présentés montrent que l'utilisation des alcools comme combustibles dans les systèmes de combustion hétérogènes nécessitent des températures de chambre plus élevées et des gouttelettes plus petites de façon à maintenir le temps de vaporisation dans un domaine acceptable.

INSTATIONÄRE VERDAMPFUNG STABILER DODEKAN- UND ALKOHOLTRÖPFCHEN IN EINER HEISSEN, NICHT REAGIERENDEN UMGEBUNG

Zusammenfassung—Es wurde ein Computer-Modell entwickelt, um die Transportgrößen für einzelne Tröpfchen während der Verdampfung in heterogenen Verbrennungssystemen zu berechnen. Ein Runge–Kutta-Verfahren vierter Ordnung ermittelt die Transportgrößen in der flüssigen Phase und im Film in Abhängigkeit von der Zeit. Das Modell berechnet den Zeitverlauf für Tröpfchengröße, Temperatur, Dampfdruck, verdampfenden Massenstrom, Wärmeübergang und Wärmestromdichte sowie integrale Werte für die verdampfte Masse und die übertragene Wärme. In dieser Untersuchung wird ein neues Näherungsverfahren zur Berechnung der Verdampfungskonstanten einzelner Tröpfchen vorgestellt. Die Ergebnisse zeigen, daß Alkohole als alternative Brennstoffe in heterogenen Verbrennungssystemen höhere Brennraumtemperaturen und kleinere Tröpfchen erfordern, um die Verdampfungsdauer innerhalb annehmbarer Grenzen zu halten.

НЕСТАЦИОНАРНОЕ ИСПАРЕНИЕ НЕПОДВИЖНЫХ КАПЕЛЬ ДОДЕКАНА И СПИРТА, ПОДВЕШАННЫХ В НАГРЕТОЙ НЕРЕАГИРУЮЩЕЙ ОКРУЖАЮЩЕЙ СРЕДЕ

Аннотация—Разработана численная модель для расчета процессов переноса при испарении единичной капли в системах гетерогенного горения. Модель позволяет рассчитать изменение во времени размера капель, температуры и давления пара, скорости испарения, интенсивности теплопереноса и величины теплового потока, а также интегральных значений переноса массы пара и тепла. Предложен новый подход к расчету постоянной испарения единичных капель. Представленные результаты показывают, что для того чтобы время испарения сохранялось в приемлемом диапазоне при использовании спиртов в качестве возможных топлив в системах гетерогенного горения, требуются более высокие температуры в камерах сгорания и капли меньших размеров.